Pertanika J. Sci. & Technol. 16 (2): 141 - 156 (2008)
ISSN: 0128-7680

Phase Behavioural Study of Palm-Based Lauryl Alcohol Ethoxylates

Lim Hong Ngee[1*], Anuar Kassim[1], Huang Nay Ming[2], Dzulkefly Kuang Abdullah[1], Abdul Halim Abdullah[1], Mohd. Ambar Yarmo[3] and Yeong Shoot Kian[4]

[1]Chemistry Department, Faculty of Science, Universiti Putra Malaysia, 43400 UPM, Serdang, Selangor, Malaysia

[2]School of Applied Physics, Faculty of Science and Technology, Universiti Kebangsaan Malaysia, 43000 Bandar Baru Bangi, Selangor, Malaysia

[3]School of Chemical Sciences and Food Technology, Faculty of Science and Technology, Universiti Kebangsaan Malaysia, 43000 Bandar Baru Bangi, Selangor, Malaysia

[4]AOTD MPOB, Lot 9 & 11, Jalan P10/14, Seksyen 10, 43650 Bandar Baru Bangi, Selangor, Malaysia

**E-mail: janet_limhn@yahoo.com*

ABSTRACT

Palm-based lauryl alcohol ethoxylates were synthesized with different chain lengths of ethylene oxide using an ethoxylation reactor. The effect of changing the ethylene oxide chain length was investigated by reacting 3, 6 and 100 moles of ethylene oxide with palm-based lauryl alcohol. The samples were labeled as $C_{12}E_3$, $C_{12}E_6$ and $C_{12}E_{100}$. The 6 moles of ethylene oxide was approximately the same length as the palm-based lauryl alcohol. The chromatograms of $C_{12}E_x$ showed less retention peaks than the standard, Brij 40 (Tetraethylene glycol dodecyl ether - $C_{12}E_4$). Fourier Transformed Infrared Spectroscopy (FTIR) displayed a strong C-O stretch at 1120 cm^{-1} which was attributed to C-O single-bond stretching of the ether group. The ternary phase diagrams for a series of olive or olein oil/water/$C_{12}E_x$ systems were investigated at 25°C. The important features of the ternary phase systems are the emulsion and the concentrated emulsion phases. Optical microscopy revealed the difference in morphology between emulsion and concentrated emulsion. The particle size of the emulsions and the concentrated emulsions were in the range of 2.635 μm to 9.175 μm and 0.694 μm to 4.764 μm, respectively. The rheological flow curves measurement of the concentrated emulsion showed crossover of the ascendant and descendant curves which indicated structural build up of the sample instead of destruction.

Keywords: Palm-based lauryl alcohol ethoxylates, ethoxylation reactor, ternary phase diagram, emulsion, concentrated emulsion

ABBREVIATIONS

$C_{12}E_x$	Palm-based lauryl alcohol ethoxylates with x as the average number of moles of ethylene oxide
$C_{12}E_3$	Palm-based lauryl alcohol with an average number of 3 moles of ethylene oxide
$C_{12}E_6$	Palm-based lauryl alcohol with an average number of 6 moles of ethylene oxide

Received : 8 August 2007
Accepted : 30 May 2008
* Corresponding Author

$C_{12}E_{100}$ Palm-based lauryl alcohol with an average number of 100 moles of ethylene oxide

$C_{12}E_4$ Brij 30 (Tetraethylene glycol dodecyl ether)

INTRODUCTION

Emulsions form the basis of a wide variety of natural and manufactured materials, including foods, pharmaceuticals, biological fluids, agrochemicals, petrochemicals, cosmetics and explosives (Schramm, 1992; Semenzato *et al.* 1994, Hyuk *et al.* 2006). Emulsions are dispersions of at least two immiscible liquids stabilized by emulsifiers, which are often surfactants (Sjoblom, 1996). The droplets of one liquid are dispersed through a second, which is the continuous phase. Surfactants, which possess polar and non-polar regions, are absorbed into the phase interfaces thus, decreasing the interfacial free energy.

In recent years, concentrated emulsions are gaining interest among researchers (Kizling and Kronberg, 2001, Becu *et al.*, 2004). The internal phase volume fraction of the concentrated emulsion is in the range of 0.8 to 0.99. These concentrated emulsions are termed biliquid foams due to their foam-like structure where the internal phase consists of polyhedral compartments. Other terminologies include high internal phase ratio emulsions (HIP) (Williams, 1991) and gel-emulsions (Ravey *et al.*, 1994), which can be either water-in-oil (W/O) or oil-in-water (O/W) type emulsions. One advantage of the highly concentrated emulsions reported by Kizling *et al.*, (2006) is their long-term stability despite very low surfactant concentrations. The characteristic resemblance of emulsions to stiff gels is attributed to its internal structure being similar to that of foams with large air/liquid ratio.

The presence of surface active agent helps reduce the tension (interfacial free energy) at the interface, thus rendering some degree of stability to the resulting emulsion system. Since the hydrophile lipophile balance (HLB) of the polyoxyethylene surfactants used in this study are higher than 10, it is highly likely that O/W type emulsions are generated, and not W/O type. The HLB value is the balance of the size and strength of the hydrophilic and lipophilic moieties of a surfactant molecule (Niraula *et al.* 2004).

Functional oils play an essential role as marketing tools to attract consumers. Olive oil is rich in monounsaturates and has resistance to oxidative change because of the presence of nutrient and non-nutrient antioxidants (Paraskevopoulou, 2005). Olein oil has 44.2% palmitic acid (16:0), 39% oleic (18:1) and 10% linoleic (18:2) acids (Solomons and Orozco, 2003). Olein oil contains tocopherol and tocotrienol content which defines Vitamin E activity (Sundram *et al.*, 2003).

The aim of this study is to examine the phase behaviour of emulsions prepared using olive or olein oil/water/$C_{12}E_x$ systems. The emulsions were characterized using an optical microscope, a particle size analyzer and a rheometer.

MATERIALS AND METHODS

Materials

Distilled water was used throughout this study for the preparation of emulsion systems. Lauryl alcohol with a purity of 99% was obtained from Cognis (M) Oleochemicals Sdn Bhd. Ethylene oxide 100% was obtained from Fluka. Potassium hydroxide 85% and citric acid were obtained from Sigma-Aldrich. Olive oil with a purity of 100% was obtained from Bronson & Jacobs. Olein oil with a purity of 99% was obtained from Moi Foods Malaysia Sdn. Bhd. Brij 40 (Tetraethylene glycol dodecyl ether - $C_{12}EO_4$) was obtained from Fluka. All chemicals were of analytical grade and were used as received.

METHODS

Synthesis of Palm–Based Lauryl Alcohol Ethoxylates ($C_{12}E_x$)

Lauryl alcohol was ethoxylated with 3, 6 and 100 moles of ethylene oxide respectively using potassium hydroxide (1 w/w %) as catalyst for the reactions. Da Vinci reactor was used for the ethoxylation process. Each reaction was left to complete for three hours at 140°C, under atmospheric pressure and stirred at 100 rpm. The pH of the synthesized liquid samples was adjusted to pH 5.0-7.0 using citric acid. The resulting liquid samples were then centrifuged at 10 000 rpm for 20 minutes to remove salt that was formed during neutralization. While for sample in solid form, no pH adjustment was required as it would be more economical to use the as-synthesized solid sample as is. Finally, both the liquid and solid samples were vacuumed at 40°C for two days to remove water. The as-synthesized samples were labeled as $C_{12}E_x$ with x as the average number of moles of ethylene oxide.

Gas Chromatography (GC)

The $C_{12}E_x$ samples were diluted with chloroform (1:500) and analysed using a Hewlett Packard gas chromatograph (GC) installed with 30 m length fused silica capillary column (HP 5) having 0.32 mm i.d. and 0.25 µm thickness. The samples were detected by flame ionization detector (FID) working at $T_{injector}$ and $T_{detector}$ = 280°C. Column temperature program was set from 50°C for 3 minutes, and then heated up to 250°C at the rate of 10°C/minute. Helium gas was used as the mobile phase at the flow rate of 1 ml/minute.

Fourier Transformed Infrared Spectroscopy (FTIR)

A Perkin Elmer Model GX type FTIR was used to investigate the structural carbonyl groups of $C_{12}E_x$. The FTIR spectrum was recorded in wavenumbers range of 500 - 4000 cm^{-1} with a resolution of 1 cm^{-1}. Sample preparation was based on KBr disk technique.

Phase Behaviour Determination

Ternary phase diagram of each of the three $C_{12}E_x$ surfactants was studied. The three components of the phase diagrams were lauryl alcohol ethoxylate as the surfactant, water as the aqueous phase and olive or olein oil as the oil phase. Six diagrams were considered namely $C_{12}E_3$/water/olive oil, $C_{12}E_6$/water/olive oil, $C_{12}E_{100}$/water/olive oil, $C_{12}E_3$/water/olein oil, $C_{12}E_6$/water/olein oil and $C_{12}E_{100}$/water/olein oil. The regions in the phase diagram were determined by titrating the oil phase into water/surfactant (w/w) in 15 mm x 100 mm test tubes. The ratios of water/surfactant were in the range of 0.11 to 9.0. $C_{12}E_{100}$ is a solid type surfactant which has to be melted by heating prior to mixing. Results of the phase diagrams were plotted. An AND analytical balance was used to determine the weight of the materials. A Thermolyne vortex was used to homogenize the samples.

Macroscopy Analysis

Organoleptic characteristics and homogeneity of emulsions were observed to identify visible instability such as creaming, flocculation or coalescence. Centrifugation was carried out for visibly stable emulsions using Hettich Retafix 32 to affirm their stability. Each emulsion sample was submitted to a cycle of 2 min at 4000 rpm at room temperature. At the end of the cycle, a macroscopic evaluation was made to observe any possible phase separation.

Particle Size Analysis

Droplet size distributions of the emulsions were measured using a Mastersizer 2000S. This system measures droplet size with the help of the light scattering technique. Owing to their opaque nature, the light scattering technique required the parent emulsion samples to be diluted. The samples were diluted at the ratio of 1:1000 with distilled water in the equipment chamber and sonicated before analysis.

Microscopy Analysis

Droplet images (size and morphology) of the emulsions were analysed by an optical microscope at room temperature (25°C). A small drop of emulsion was placed onto the microscope slide and carefully covered. After equilibration for 1 min, photomicrographs (x100 magnification) were taken using the optical microscope (Nikon, Japan) equipped with a digital camera (XLi, USA). The size of the emulsion droplets was measured using an I-Solution Image Analyzer (IMT Inc., Canada).

Rheological Study

A Rheometer (PAAR Physica MCR 300), operated by a Rheoplus software, was used to evaluate steady–shear analysis of emulsion and concentrated emulsion. The analysis was carried out using a cone and plate geometry. The plate gap was set to 0.125 mm. Steady-state analysis was used for characterization of the emulsion and concentrated emulsion behaviour under shear. Measurements were carried out on emulsion samples to determine the role of shear in the eventual destruction of the emulsion. The controlled shear rate (CSR) procedure was selected for flow curve evaluation. Values of maximal and minimal apparent viscosity were used for characterization of the samples for flow analysis. The speed was varied to produce the two curves (ascendant and descendant). Flow index data and viscosity were obtained at different times during the test. All samples were tested at 25 ± 0.2°C.

RESULTS AND DISCUSSION

Gas Chromatography (GC)

Fig. 1 shows the chromatograms of lauryl alcohol, Brij 30 ($C_{12}E_4$), $C_{12}E_3$, $C_{12}E_6$ and $C_{12}E_{100}$. Chromatograms having less retention peaks imply higher purity samples. The chromatogram of lauryl alcohol displayed only one retention peak at 15 min (*Fig. 1* (a)). Brij 30 ($C_{12}E_4$) was used as a standard for the as-synthesized palm-based lauryl alcohol ethoxylates. The chromatogram of Brij 30 ($C_{12}EO_4$) consisted of eleven significant retention peaks which implied that the number of moles of ethylene oxide for the standard was taken as an average (*Fig. 1* (b)). The chromatogram also had a retention peak at 15 min which shows that the lauryl alcohol of the standard had not undergone a full conversion during the reaction. The chromatograms of $C_{12}E_3$ (*Fig. 1* (c)), $C_{12}E_6$ (*Fig. 1* (d)) and $C_{12}E_{100}$ (*Fig. 1* (e)) displayed less retention peaks than Brij 30 ($C_{12}E_4$) which shows that the as-synthesized samples had higher purity than the standard. Moreover, the lauryl alcohol of $C_{12}E_3$, $C_{12}E_6$ and $C_{12}E_{100}$ had been fully converted during reaction as there was no retention peak at 15 min.

Fourier Transformed Infrared Spectroscopy (FTIR)

In *Fig.* 2, the spectrum of lauryl alcohol was differentiated from the rest of the ethoxylated standard and as-synthesized samples by the medium stretch at 1050cm^{-1}

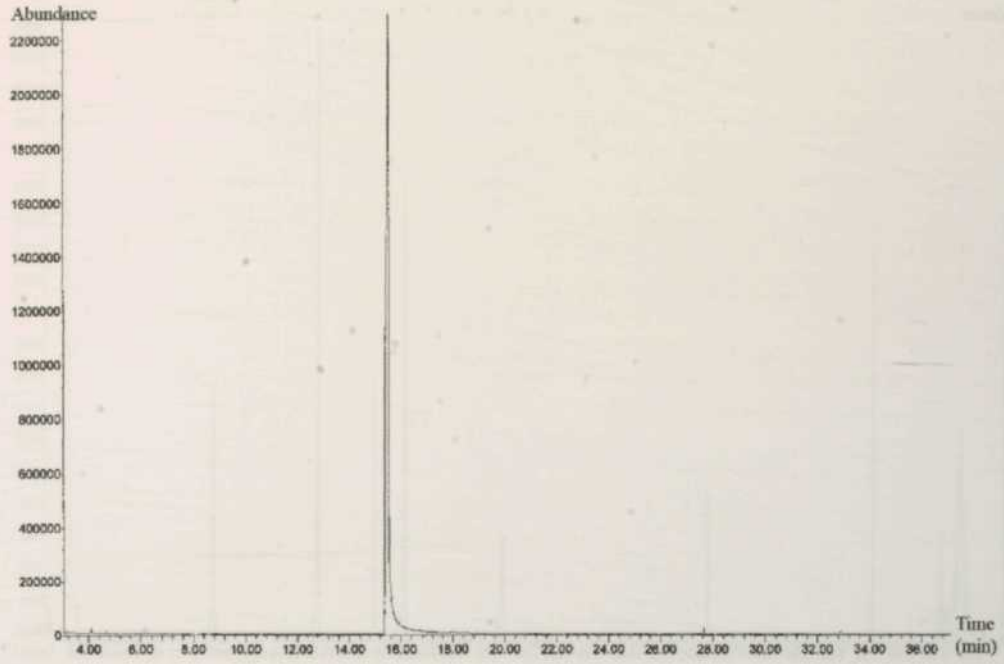
Abundance
2200000
2000000
1800000
1600000
1400000
1200000
1000000
800000
600000
400000
200000
0
4.00 6.00 8.00 10.00 12.00 14.00 16.00 18.00 20.00 22.00 24.00 26.00 28.00 30.00 32.00 34.00 36.00
Time (min)

Fig. 1 (a)

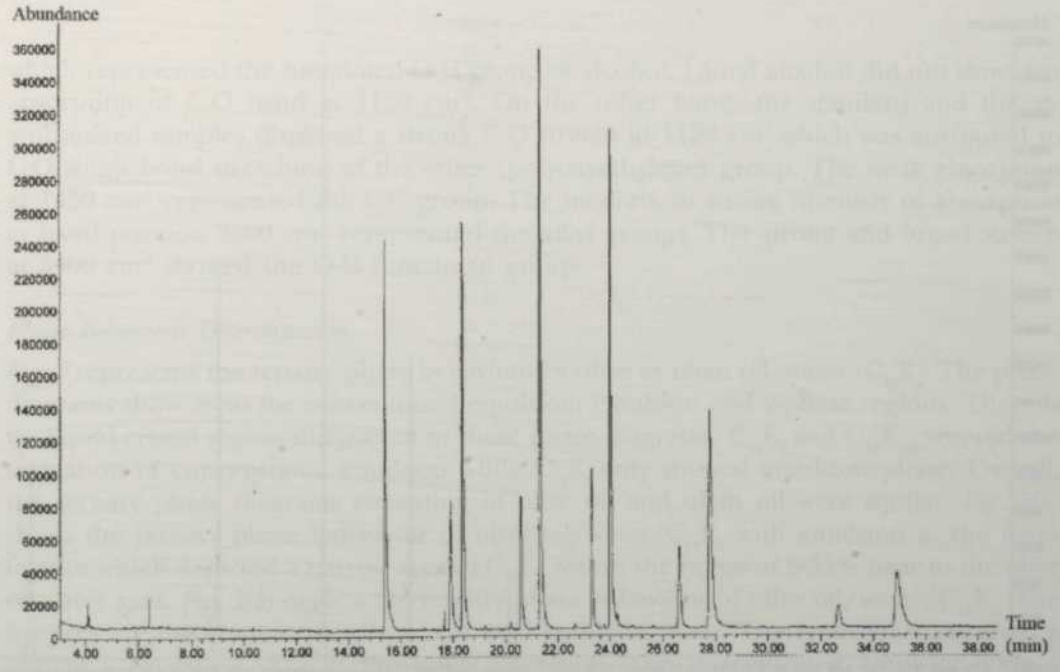
Abundance
360000
340000
320000
300000
280000
260000
240000
220000
200000
180000
160000
140000
120000
100000
80000
60000
40000
20000
0
4.00 6.00 8.00 10.00 12.00 14.00 16.00 18.00 20.00 22.00 24.00 26.00 28.00 30.00 32.00 34.00 36.00 38.00
Time (min)

Fig. 1 (b)

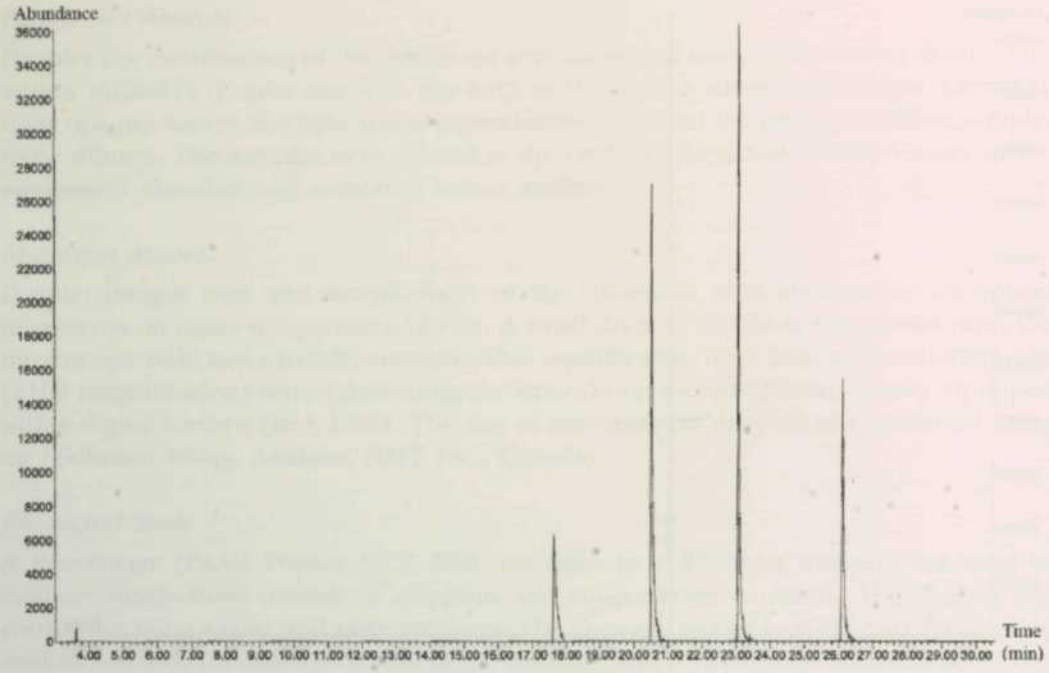
Abundance
36000
34000
32000
30000
28000
26000
24000
22000
20000
18000
16000
14000
12000
10000
8000
6000
4000
2000
0
4.00 5.00 6.00 7.00 8.00 9.00 10.00 11.00 12.00 13.00 14.00 15.00 16.00 17.00 18.00 19.00 20.00 21.00 22.00 23.00 24.00 25.00 26.00 27.00 28.00 29.00 30.00
Time
(min)

Fig. 1 (c)

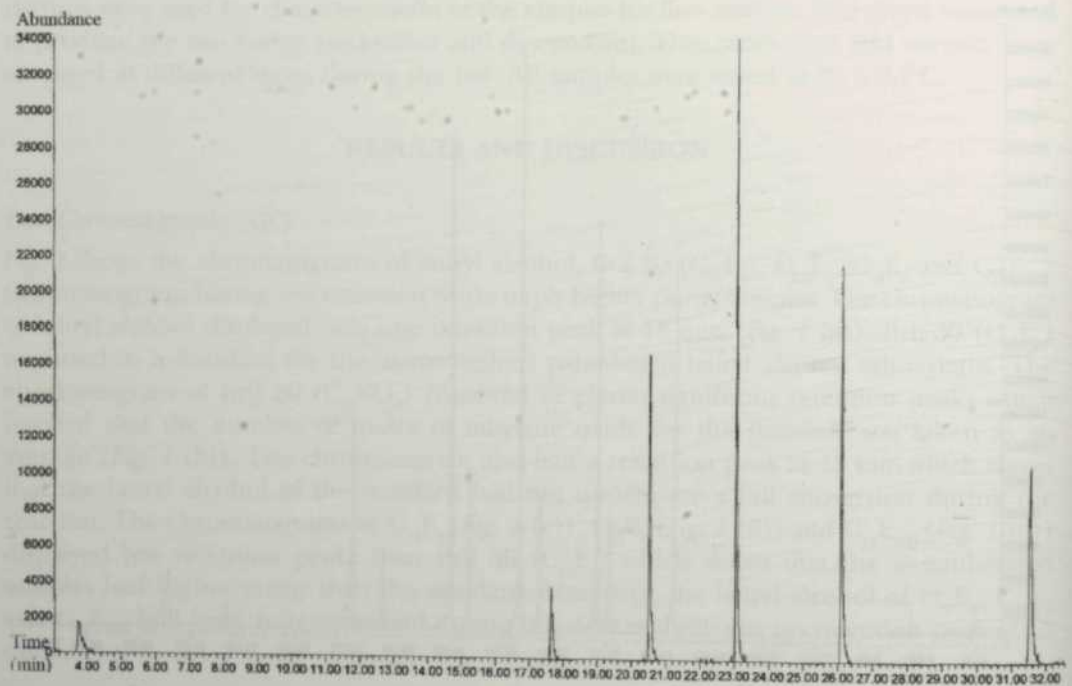
Abundance
34000
32000
30000
28000
26000
24000
22000
20000
18000
16000
14000
12000
10000
8000
6000
4000
2000
Time
(min)
4.00 5.00 6.00 7.00 8.00 9.00 10.00 11.00 12.00 13.00 14.00 15.00 16.00 17.00 18.00 19.00 20.00 21.00 22.00 23.00 24.00 25.00 26.00 27.00 28.00 29.00 30.00 31.00 32.00

Fig. 1 (d)

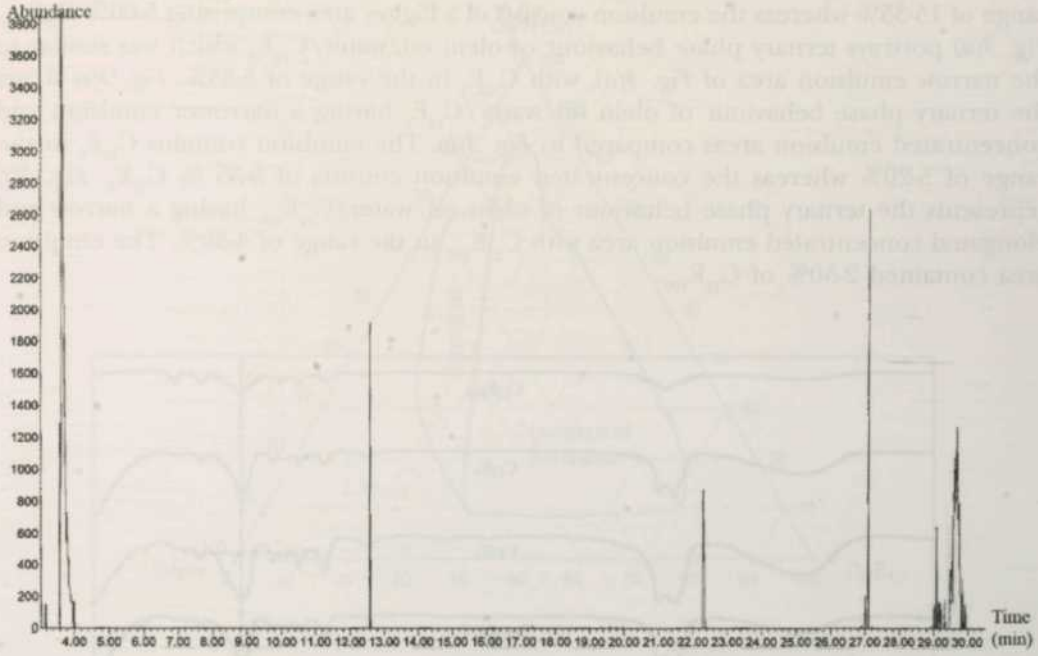

Fig. 1: Chromatograms of (a) lauryl alcohol, (b) standard, Brij 30 ($C_{12}E_4$), (c) $C_{12}EO_3$, (d) $C_{12}EO_6$ and (e) $C_{12}EO_{100}$

which represented the functional O-H group of alcohol. Lauryl alcohol did not show any absorption of C-O band at 1120 cm^{-1}. On the other hand, the standard and the as-synthesized samples displayed a strong C-O stretch at 1120 cm^{-1} which was attributed to C-O single-bond stretching of the ether (polyoxyethylene) group. The weak absorption at 1450 cm^{-1} represented the C-C group. The medium to strong intensity of absorption at band position 2800 cm^{-1} represented the alkyl groups. The strong and broad stretch at 3400 cm^{-1} showed the O-H functional group.

Phase Behaviour Determination

Fig. 3 represents the ternary phase behaviour of olive or olein oil/water/$C_{12}E_x$. The phase diagrams show areas for concentrated emulsion, emulsion and 2-phase regions. There is no liquid crystal region discovered in these phase diagrams. $C_{12}E_6$ and $C_{12}E_{100}$ showed the formation of concentrated emulsion while $C_{12}E_3$ only showed emulsion phase. Overall, the ternary phase diagrams consisting of olive oil and olein oil were similar. *Fig. 3(a)* shows the ternary phase behaviour of olive oil/water/$C_{12}E_3$ with emulsion as the main feature which depicted a narrow area of $C_{12}E_3$ within the range of 5-35% near to the olive oil-water axes. *Fig. 3(b)* depicts the ternary phase behaviour of olive oil/water/$C_{12}E_6$. The features are the emulsion and concentrated emulsion areas. The emulsion comprised a narrow area with $C_{12}EO_6$ in the range of 3-35%. The concentrated emulsion gave a smooth and stiff texture with $C_{12}E_6$ in the range of 8-70%. *Fig. 3(c)* represents the ternary phase behaviour of olive oil/water/$C_{12}E_{100}$ featuring the emulsion and concentrated emulsion areas. The concentrated emulsion covers only a small area with $C_{12}E_{100}$ in the

range of 15-35% whereas the emulsion consists of a bigger area comprising 5-60% $C_{12}E_{100}$. *Fig. 3(d)* portrays ternary phase behaviour of olein oil/water/$C_{12}E_3$ which was similar to the narrow emulsion area of *Fig. 3(a)*, with $C_{12}E_3$ in the range of 5-35%. *Fig. 3(e)* shows the ternary phase behaviour of olein oil/water/$C_{12}E_6$ having a narrower emulsion and concentrated emulsion areas compared to *Fig. 3(b)*. The emulsion contains $C_{12}E_6$ in the range of 5-20% whereas the concentrated emulsion consists of 5-35 % $C_{12}E_6$. *Fig. 3(f)* represents the ternary phase behaviour of olein oil/water/$C_{12}E_{100}$ having a narrow and elongated concentrated emulsion area with $C_{12}E_{100}$ in the range of 4-30%. The emulsion area contained 2-50% of $C_{12}E_{100}$.

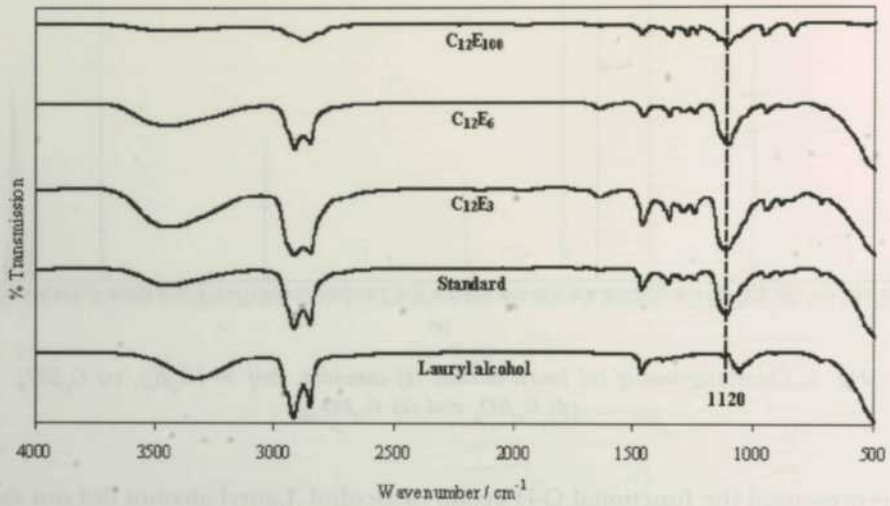

Fig. 2: FTIR spectrum of palm-based lauryl alcohol, Brij 40 ($C_{12}EO_4$) as a standard and as-synthesized samples of $C_{12}EO_3$, $C_{12}EO_6$ and $C_{12}EO_{100}$

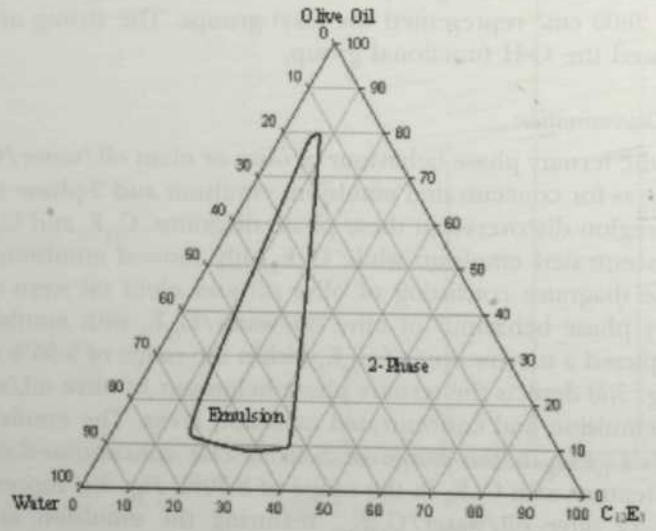

Fig. 3 (a)

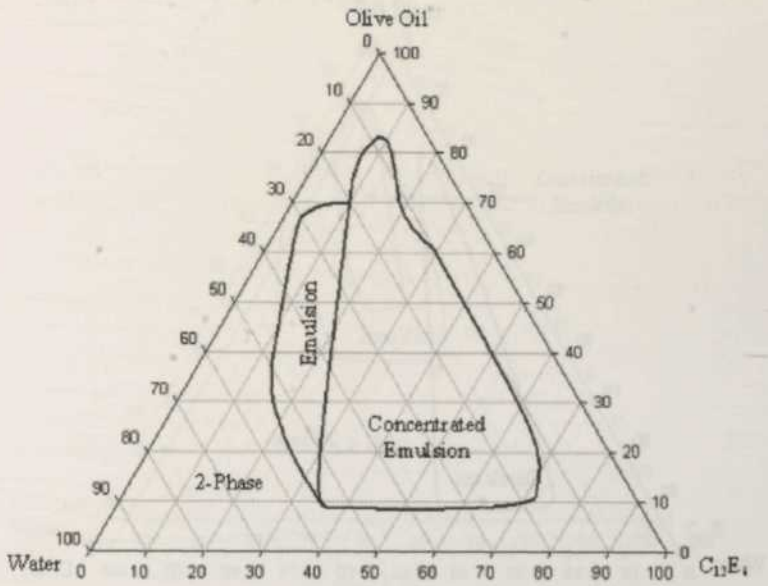
Olive Oil
Emulsion
Concentrated Emulsion
2-Phase
Water
$C_{12}E_4$

Fig. 3 (b)

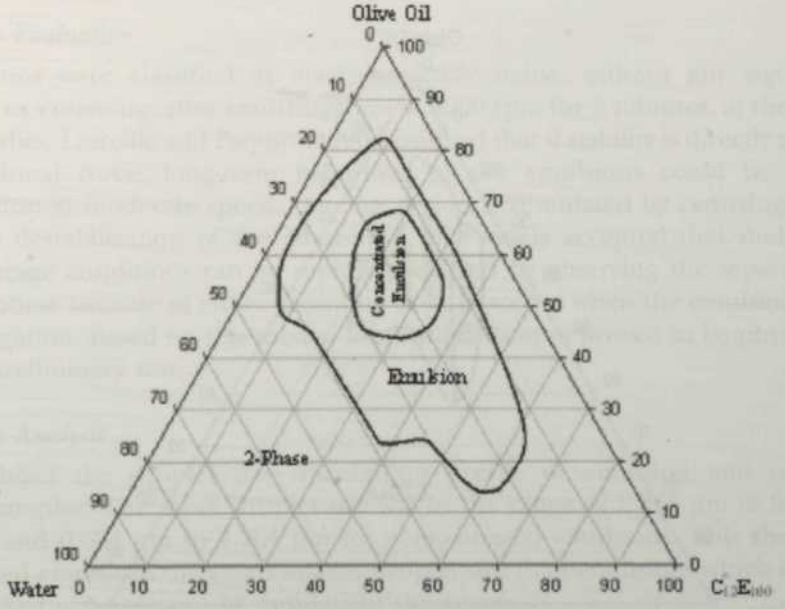
Olive Oil
Concentrated Emulsion
Emulsion
2-Phase
Water
$C_{12}E_{10}$

Fig. 3 (c)

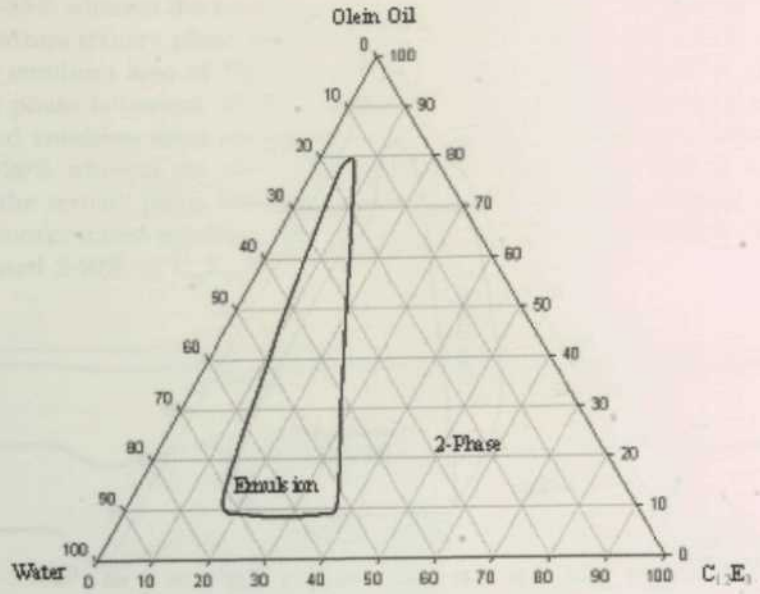
Olein Oil
Water
$C_{12}E_4$
Emulsion
2-Phase

Fig. 3 (d)

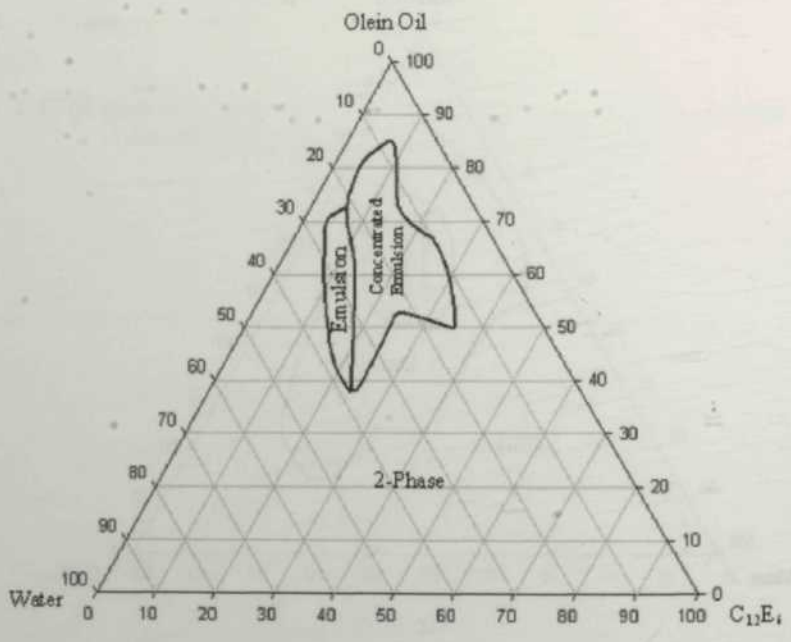
Olein Oil
Water
$C_{12}E_4$
Emulsion
Concentrated Emulsion
2-Phase

Fig. 3 (e)

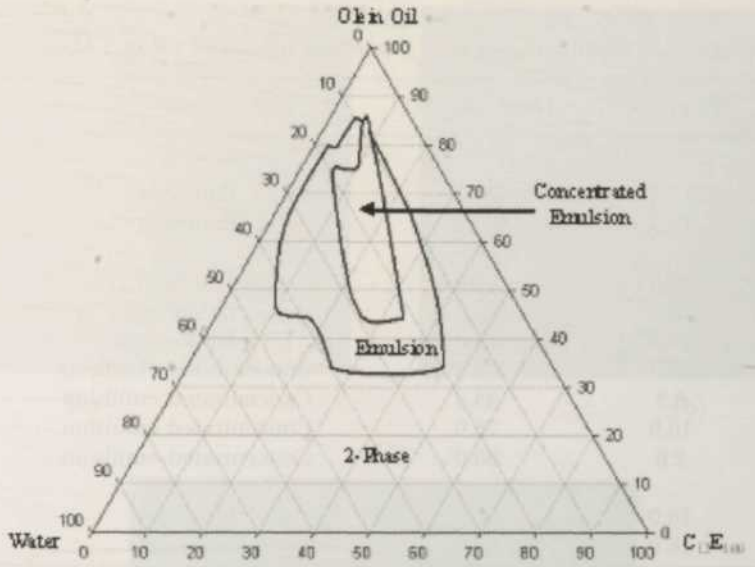

Fig. 3 (f)

Fig. 3: Ternary phase diagrams of (a) $C_{12}EO_3$/water/olive oil, (b) $C_{12}EO_6$/water/olive oil, (c) $C_{12}EO_{100}$/ water/olive oil, (d) $C_{12}E_3$/water/olein oil, (e) $C_{12}E_6$/water/olein oil and (f) $C_{12}E_{100}$/water/olein oil

Macroscopic Evaluation

All emulsions were classified as macroscopically stable, without any signs of phase separation or creaming, after centrifugation at 4000 rpm for 2 minutes, at the start of the stability studies. Latreille and Paquin (1990) assumed that if stability is directly proportional to gravitational force, long-term behaviour of the emulsions could be assessed by centrifugation at moderate speeds. Ageing period is stimulated by centrifugation which accelerates destabilization of the emulsions. It is widely accepted that shelf life under normal storage conditions can be rapidly predicted by observing the separation of the dispersed phase because of either creaming or coalescence when the emulsion is exposed to centrifugation. Based on this theory, the emulsions were proven to be physically stable after the preliminary test.

Particle Size Analysis

Table 1 shows the droplet size distribution profile of emulsion and concentrated emulsion samples. The mean droplet size was in the range of 2.635 μm to 9.175 μm for emulsions and 0.694 μm to 4.764 μm for concentrated emulsions. This shows that the concentrated emulsions displayed smaller droplet size than emulsions which is due to the closely packed arrangement of droplets in the system.

Microscopic Evaluation

Fig. 4(a) depicts the emulsion of the $C_{12}E_6$/water/olein oil (2.5%/22.5%/75.0%) system observed under an optical microscope. The average size of the emulsion oil droplets by counting at least 1000 droplets using image analysis software was 6.45 ± 1.39 μm, which

TABLE 1
Average droplet size distribution of $C_{12}E_x$/water/oil measured using a Mastersizer 2000S

$C_{12}E_x$ (%)	Water (%)	Olive Oil (%)	Type	Size (μm)
$C_{12}E_3$				
4.3	17.0	78.7	Emulsion	3.06
6.0	14.0	80.0	Emulsion	2.64
$C_{12}E_6$				
2.5	22.5	75.0	Emulsion	5.77
5.0	20.0	75.0	Emulsion	5.36
7.5	17.5	75.0	Emulsion	3.08
8.9	13.3	77.8	Concentrated emulsion	2.15
8.3	8.3	83.4	Concentrated emulsion	1.12
15.0	10.0	75.0	Concentrated emulsion	1.47
18.0	2.0	80.0	Concentrated emulsion	0.69
$C_{12}E_{100}$				
2.0	18.0	80.0	Emulsion	9.18
4.0	16.0	80.0	Emulsion	7.28
$C_{12}E_x$ (%)	Water (%)	Olein Oil (%)	Type	Size (μm)
$C_{12}E_3$				
5.0	20.0	75.0	Emulsion	3.33
6.0	14.0	80.0	Emulsion	2.76
$C_{12}E_6$				
2.5	22.5	75.0	Emulsion	5.99
5.0	20.0	75.0	Concentrated emulsion	4.76
4.8	11.3	83.9	Concentrated emulsion	2.69
5.7	8.6	85.7	Concentrated emulsion	1.34
$C_{12}E_{100}$				
2.0	18.0	80.0	Emulsion	7.82
4.0	16.0	80.0	Emulsion	6.58
4.3	10.0	85.7	Emulsion	5.27
5.7	8.6	85.7	Concentrated emulsion	3.65

was similar to the particle size measured by the light scattering method. *Fig. 4(b)* shows the droplets arrangement of concentrated emulsion of the $C_{12}EO_6$/water/olive oil (8.3%/8.3%/83.4%) system. The droplets were found to be closely arranged with the oil droplets dispersed in the continuous water phase. Oil droplets are confirmed as the dispersed phase through a simple microslide capillary test by diffusing water into the concentrated emulsion observed under an optical microscope. The droplets of oils were released into water as soon as it was diluted. *Fig. 4(c)* shows oil droplets dispersed in water when the concentrated emulsion was diluted by water using the capillary method. The average size of the oil droplets for the concentrated emulsion is 1.01 ± 0.17 μm, which is close to the particle size measured by the light scattering method.

Rheological Study

Flow experiment involves measuring the shear rate as a function of shear stress. Continuous shear experiments measure the ability of each system to resist structural

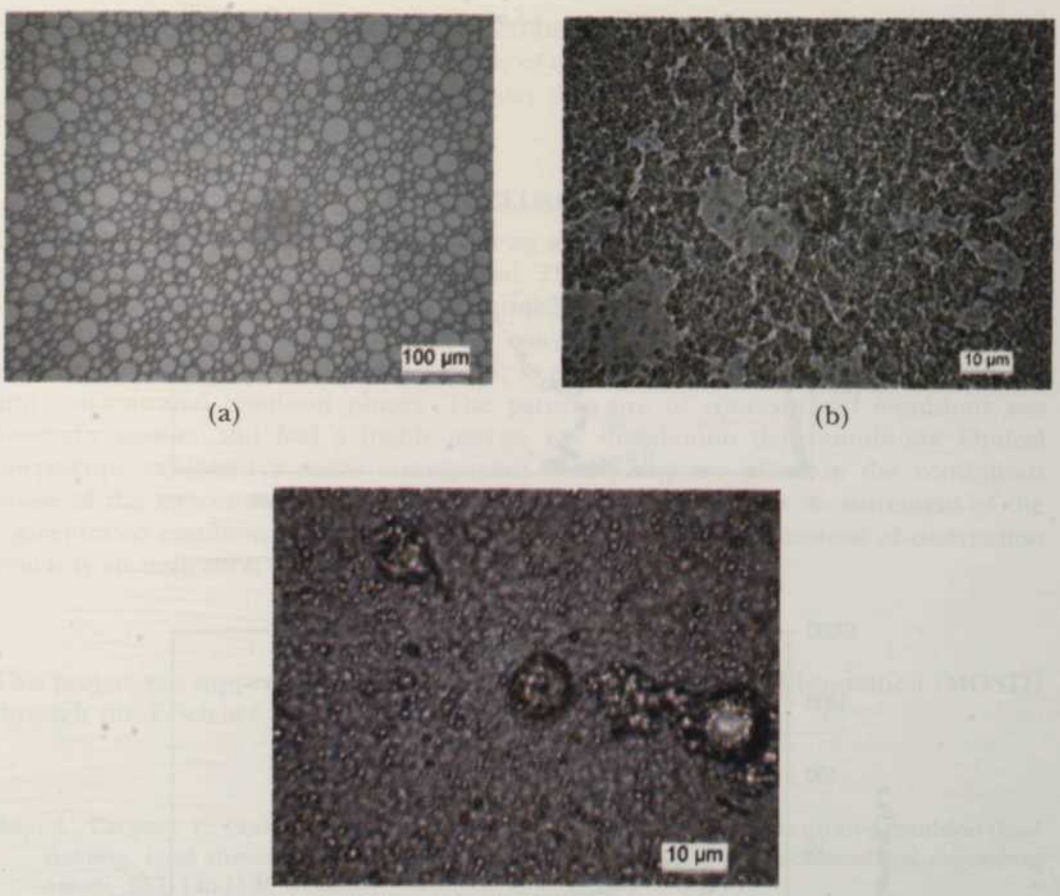

(a) (b)

(c)

Fig. 4: Morphologies of the (a) $C_{12}E_6$/water/olein oil emulsion, (b) $C_{12}E_6$/water/olive oil concentrated emulsion and (c) dilution of concentrated emulsion from (b) in water

breakdown during the standardized shearing procedure. The resulting rheogram shows three sections: the ascendant curve, the peak hold region and the descendant curve. Both the ascendant and descendant flow curves in *Fig. 5(a)* indicated shear thinning. The smooth flow curve (1) indicated a stable emulsion. In contrast, the concentrated emulsion indicated by flow curve (2) was complex and different from flow curve (1). The ascendant and descendant curves cross over implies that the shearing cycle itself might cause structural build-up, rather than destruction (Ribeiro *et al.*, 2003). If on a shear rate-shear stress plot for a material, the data are extrapolated to zero shear rate and the plot appears to cut the shear stress axis on the graph at a positive stress value, then the material is said to possess a yield stress. In practice, it means that a certain mild force must be applied before the system will flow (Strivens, 1987). A yield stress of approximately 25 Pa is observed in flow curve (2). The hysteresis loop can be interpreted as the stability of the droplets. The ascendant and descendant curves in flow curves (1) were almost the same. This means that the shear does not induce irreversible structural changes (Terrisse *et al.*, 1993).

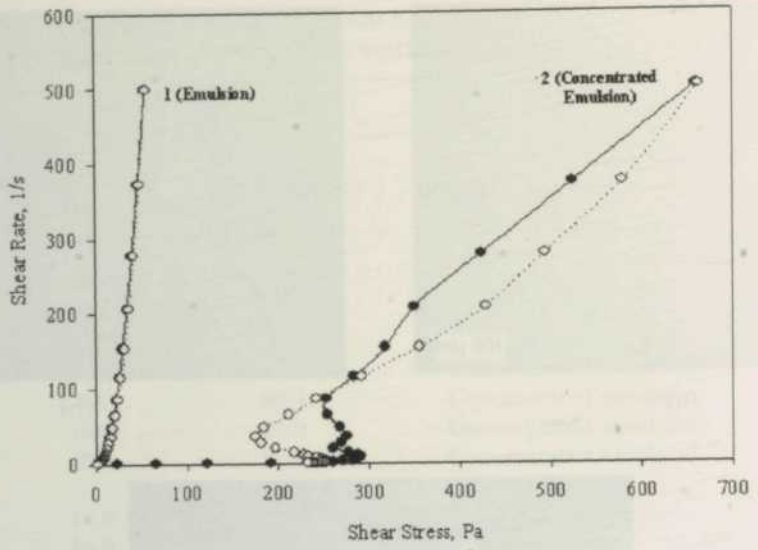

(a)

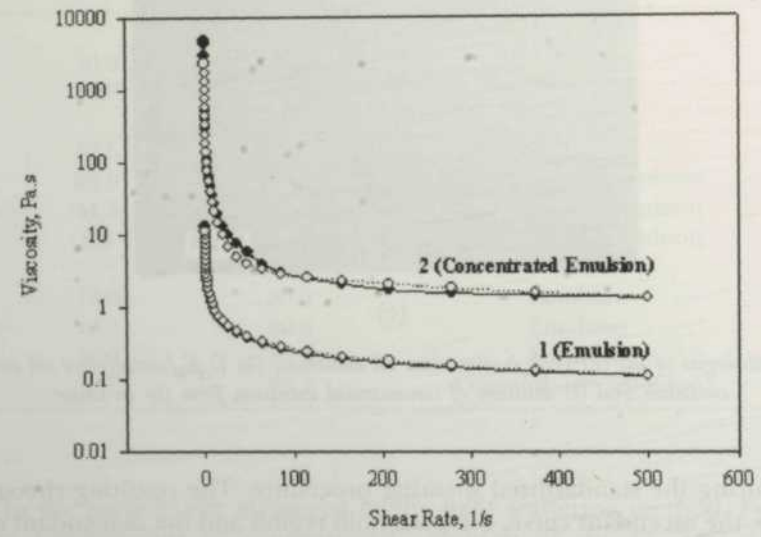

(b)

Fig. 5: (a) Flow curves of the olein oil/water/$C_{12}E_6$ emulsion (1) and olive oil/water/$C_{12}E_6$ concentrated emulsion (2) with • (closed circle) - ascendant curve and ? (open circle) – descendant curve, (b) Viscosity for emulsion of the olein oil/water/$C_{12}E_6$ system (1) and concentrated emulsion of the olive oil/water/$C_{12}E_6$ system (2) with • - descendant curve and ∘ – ascendant curve

Viscosity values provide a comparison of the resistance to structural breakdown. Both the curves in *Fig. 5(b)* decreased in viscosity as shear rate increased. This feature also indicated shear thinning behaviour. The important criteria of shear thinning materials are that: (i) the apparent viscosity decreases with increasing shear rate (or shear stress) values, and (ii) the apparent viscosity value at a given shear rate value is independent of the shear history of the sample. In curve (2), the high apparent viscosity value indicated

that the concentrated emulsion was thicker and more resistant to structure breakdown (Ribeiro *et al.*, 2003). The apparent viscosity of concentrated emulsion containing smaller droplets (1.120 μm) was significantly greater than emulsion containing larger droplets (5.987 μm).

CONCLUSIONS

Palm-based lauryl alcohol ethoxylates with an average number of 3, 6 and 100 moles of ethylene oxide were successfully synthesized. The different concentrations of oil/water/$C_{12}E_x$ determine the type of emulsion formed whether normal or concentrated. The ternary phase diagrams of oil/water/$C_{12}E_3$ consisted of only an emulsion area while the ternary phase diagrams of oil/water/$C_{12}E_6$ & oil/water/$C_{12}E_{100}$ demonstrated emulsion and concentrated emulsion phases. The particle size of concentrated emulsions was generally smaller and had a highly narrow size distribution than emulsions. Optical microscope exhibited a dense arrangement of the disperse phase in the continuous phase of the concentrated emulsions. The rheological flow curves measurement of the concentrated emulsion implied that there was structural build up instead of destruction which is an indication of high sample stability.

ACKNOWLEDGEMENTS

This project was supported by Ministry of Science, Technology and Innovation (MOSTI) through the E-Science Fund grant number 03-01-04-SF-0407.

REFERENCES

Becu, L., Grondin, P., Colin, A. and Manneville, S. (2004). How does a concentrated emulsion flow? Yielding, local rheology and wall slip. *Colloids and Surfaces A: Physicochemical and Engineering Aspects, 263*, 146-152.

Hyuk, S.Y., Mazda, O, Hyeon, Y.L., Jin, C.K., Seok, M.K., Jung, E.L., Ick, C.K., Jeong, H., Yu, S.J. and Seo, Y.J. (2006). In vivo gene therapy of type I diabetic mellitus using a cationic emulsion containing an Epstein Barr Virus (EBV) based plasmid vector. *Journal of Controlled Release, 112*, 139–144.

Kizling, J. and Kronberg, B. (2001). On the formation of concentrated stable W/O emulsions. *Advances in Colloid and Interface Sciences, 89-90*, 395-399.

Kizling, J., Kronberg, B. and Eriksson, J. C. (2006). On the formation and stability of high internal phase O/W emulsions. *Advances in Colloid and Interface Science, 123-126*, 295-302.

Latreille, B. and Paquin, P. (1990). Evaluation of emulsion stability by centrifugation with conductivity measurements. *Journal of Food Science, 55*, 1666-1668.

Niraula, B., Tan, C.K., Tham, K.C. and Misran, M. (2004). Rheology properties of glycopyranoside stabilized oil-water emulsions: Effect of alkyl chain length and bulk concentration of the surfactant. *Colloids and Surfaces A: Physicochemical and Engineering Aspects, 251*, 117-132.

Paraskevopoulou, A., Boskou, D. and Kiosseoglou, V. (2005). Stabilization of olive oil-lemon juice emulsion with polysaccharides. *Food Chemistry, 90*, 627–634.

Ravey, J.C., Stébé, M.J. and Sauvage, S. (1994). Water in fluorocarbon gel emulsions: Structures and rheology *Colloids and Surfaces A, Physicochemical and Engineering Aspects, 91*, 237-257.

Ribeiro, H. M., Morais, J. A. and Eccleston, G.M. (2004). Structure and rheology of semisolid o/w creams containing cetyl alcohol/non-ionic surfactant mixed emulsifier and different polymers. *International Journal of Cosmetic Science, 26,* 47-59.

Schramm, L.L. (2004) Emulsions: fundamentals and applications in the petroleum industry. American Chemical Society, Washington, D. C.

Semenzato, A., Bau, A., Dall'aglio, C., Nicolini, M. and Bettero, A. (1994). Stability of Vitamin A palmitate in cosmetic emulsions: influence of physical parameters. *International Journal of Cosmetic Science, 16*(4), 139–147.

Sjoblom, J. (1996). *Emulsions and Emulsion Stability. Surfactant Science Series Vol. 61.* New York: Marcel Dekker.

Solomons, N. W. and Orozco, M. (2003). Alleviation of vitamin A deficiency with palm fruit and its products. *Asia Pacific Journal of Clinical Nutrition, 12*(3), 373-384.

Strivens, T. A. (1987). An introduction to rheology. In R. Lambourne (Ed.), *Paint and Surface Coatings, Theory and Practice* (pp. 559-560). London: Ellis Horwood.

Sundram, K., Sambanthamurthi, R., Tan, Y.A. (2003). Palm fruit chemistry and nutrition. *Asia Pacific Journal of Clinical Nutrition, 12 (3),* 355-362.

Terrisse, I., Seiller, M., Rabaron, A., Gossiord, J.L. (1993). Rheology: How to characterize and to predict the evolution of W/O/W multiple emulsions. *International Journal of Cosmetic Science, 15,* 53-62.

Williams, J.M. (1991). High internal phase water-in-oil emulsions: Influence of surfactants and cosurfactants on emulsion stability and foam quality or gel-emulsions. *Langmuir,* 7, 1370-1377.